Journal of Energy

VOLUME 75 Number 3 | 2026

journal homepage: http://journalofenergy.com/

# An Investigation on the Effect of Frequency Dependent Inductance Calculation on High Frequency Modeling of Transformer Winding

Morteza Eslamian, Ebrahim Rahimpour, Kabir Sethi

***Summary*** **— A common approach for analyzing transformer transients is to construct a detailed winding model composed of inductive and capacitive elements. Although equivalent circuits with constant inductances remain widely used in transient studies, extensive research shows that such models lack sufficient accuracy for predicting internal winding resonances which exhibit significant discrepancies in the time domain as well. To overcome this limitation, it is necessary to incorporate the frequency dependent behavior of winding inductances, capturing proximity effects and eddy current losses within the conductors. A fully frequency dependent model requires computing parameters over a broad frequency range and performing frequency domain analysis, which is computationally demanding. In contrast, constant inductance models remain attractive due to their mathematical simplicity and the availability of efficient, direct time domain solution methods. These methods are especially advantageous when nonlinear components, such as zinc oxide surge arresters, are incorporated internally. Considering these factors, this paper proposes a method to enhance constant inductance models by selecting an appropriate inductance matrix computed at a higher frequency, thereby incorporating essential frequency dependent effects. To this end, winding responses are evaluated using multiple inductance matrices derived at different computation frequencies, and it is shown that choosing the frequency based on the spectral content of the applied impulse waveform can noticeably improve the model accuracy. The proposed approach is validated through Frequency Response Analysis (FRA) and Recurrent Surge Oscillation (RSO) measurements performed on the active part of a 250 MVA power transformer. Measurements include both time and frequency domain voltage responses obtained from internal points of the high voltage winding. This paper provides a comprehensive description of the method, including the construction of the equivalent model, parameter determination, and experimental verification.**

***Keywords*** **— Transformer winding, frequency dependency, inductance matrix, frequency response, FRA, RSO, fast transients**

(Corresponding author: Morteza Eslamian)

Morteza Eslamian and Kabir Sethi are with Hitachi Energy, Bad Honnef, Germany (email: morteza.eslamian@hitachienergy.com, kabir.sethi@hitachienergy.com)

Ebrahim Rahimpour is with Technical University of Applied Sciences Würzburg-Schweinfurt (THWS), Schweinfurt, Germany (email: Ebrahim.rahimpour@thws.de)

## I. Introduction

Transient analysis of transformer windings plays a crucial role in evaluating the electrical stress imposed on winding insulation during switching operations and lightning impulses in power systems. Such transient overvoltages are characterized by steep wavefronts and complex oscillatory behavior, which lead to non-uniform voltage distribution along the winding and severe local insulation stress. Accurate prediction of these internal voltage responses is therefore essential for transformer design and insulation coordination studies. Transformer windings constitute a distributed electromagnetic system formed by inductances and capacitances associated with individual turns. This distributed nature contributes to multiple resonance modes whose frequencies depend on winding geometry, conductor arrangement, and material properties.

Various modelling approaches have been proposed in the literature to capture the high-frequency and fast transient behavior of transformer windings. These approaches can be broadly classified into three categories: white-box, grey-box, and black-box models, depending on the level of physical detail and reliance on experimental data. White-box models are based on detailed physical representations of the transformer geometry, materials, and electromagnetic phenomena [1]–[6]. In these models, windings are discretized into multiple elements, and parameters such as inductances, capacitances, and resistances are derived analytically or using field computations. Transmission-line-based winding models and frequency-dependent lumped-parameter circuits belong to this category [7]–[9]. Black-box models, in contrast, rely entirely on terminal measurements such as frequency response analysis (FRA) or broadband impulse tests. These models represent the transformer as a network or transfer function identified from measured data, without explicitly modelling the internal physical structure [10], [11]. Grey-box models represent a compromise between purely physical and purely measurement-based approaches. In this class of models, the transformer winding is described using a simplified physical structure, while key parameters are extracted or tuned using measurement data [12].

A widely used approach for transient analysis involves subdividing transformer windings into smaller elements and constructing an equivalent circuit based on analytically or FEM-based calculated inductances and capacitances. In conventional implementations, the inductance matrix is calculated assuming uniform current distribution within conductors, resulting in constant, frequency-independent inductance values that effectively represent the zero-frequency condition. Despite their simplicity and computational



Morteza Eslamian, Ebrahim Rahimpour, Kabir Sethi, An Investigation on the Effect of Frequency Dependent Inductance Calculation on High Frequency Modeling of Transformer Winding, Journal of Energy, vol. 75 Number 3 (2026), 12–28
https://doi.org/10.37798/2026753754

© 2026 Copyright for this paper by authors. Use permitted under Creative Commons Attribution-NonCommercial (CC BY-NC) 4.0 International License

efficiency, such constant-inductance models have been shown to lack sufficient accuracy in predicting internal resonances and voltage responses at higher frequencies, particularly above several tens or hundreds of kilohertz. The limitations of zero frequency inductance models are mainly associated with the neglect of frequency-dependent effects including the eddy current losses in winding conductors. At elevated frequencies, these phenomena significantly alter both the current distribution and the leakage magnetic field, leading not only to increased losses but also to changes in the effective inductances of winding elements which result in shifts in resonance frequencies as a result.

In the previous work, the authors investigated the voltage responses of transformer windings using frequency-varying inductance models in the frequency–domain [8]. Although that approach provided accurate insight into the resonance behaviour of large power transformer windings, it required frequency-domain computations and inverse transformations to obtain time-domain responses as well. Thus, frequencydomain modelling approaches remain computationally intensive from a practical engineering perspective. Furthermore, they become less suitable when nonlinear elements, such as zinc oxide surge arresters, are included in the network, since nonlinear behavior cannot be directly handled in the frequency–domain. In contrast, time-domain models with constant parameters offer fast solution times, straight forward implementation, and natural compatibility with nonlinear components. For these reasons, constantinductance winding models continue to be widely used in transient studies, despite their known shortcomings at high frequencies.

A practical compromise between modelling accuracy and computational efficiency is achieved by employing constant inductance matrices calculated not at zero frequency, but at higher frequencies that more closely represent the dominant spectral content of the applied voltage waveform. By doing so, important high-frequency effects related to eddy currents are implicitly taken into account while preserving the simplicity of time-domain simulations. The selection of an appropriate calculation frequency for the inductance matrix, however, depends strongly on the characteristics of the excitation waveform. For instance, full lightning impulse waveforms typically contain significant spectral components up to approximately 200 kHz, whereas chopped impulse waveforms may include components approaching or exceeding 1 MHz. The present study systematically examines the influence of the calculation frequency on the predicted time and frequency responses of transformer windings when using a constant inductance model. Inductance matrices are computed at various frequencies and applied in the winding model to assess their ability to reproduce transient voltage response.

The verifications are done by experimental measurements conducted on the active part of a 250 MVA, 525/154/66 kV power transformer. Frequency-domain voltage responses were measured at internal points of the high-voltage winding and compared with simulation results obtained using inductance matrices calculated at different frequencies. The findings confirm that selecting the inductance calculation frequency in accordance with the excitation waveform provides an effective and practical means of improving transformer transient simulations without sacrificing computational efficiency or compatibility with nonlinear modelling requirements.

## II. Impedance Calculation

Inductance can be computed using analytical methods or finite element method (FEM). Analytical formulas assume a uniform current distribution and are based on Fourier series analysis inside the core window and Fourier transform analysis outside the core window. In the past, air-core models were commonly used under the assumption that high-frequency flux does not enter the core. However, later studies showed that the magnetic core still affects winding impedances at high frequencies by altering the leakage-flux distribution and contributing to damping due to the core losses [13]. Analytical methods cannot capture the frequency-dependent current distribution in conductors or the resulting changes in the external magnetic field, making them unsuitable for modelling frequency-dependent behavior. Typically, inductance is calculated at zero frequency, and frequency-dependent losses are approximated using empirical damping coefficients. The accuracy of this method can be enhanced to a large extent if the inductance matrix can be calculated at higher frequencies.

Accurate representation of transformer winding impedance at high frequencies requires accounting for frequency dependent phenomena such as eddy current losses including skin and proximity effects in conductive and magnetic materials. These effects demonstrate themselves as both an increase in effective resistance and a change of the leakage inductance as frequency increases. To capture these phenomena in a unified and physically consistent manner, the impedance matrix of the winding elements is calculated using a complex permeability formulation [14]–[17]. In this approach, the magnetic permeability of conductive and magnetic regions is expressed as a complex, frequency-dependent quantity

$$\mu^*(\omega) = \mu'(\omega) - j\mu''(\omega) \tag{1}$$

where μ′ represents the energy storage capability of the magnetic field, and μ″ accounts for magnetic losses associated with induced eddy currents and hysteresis effects. By incorporating $\mu^*(\omega)$ into the field solution, both resistive and inductive effects are inherently included in the resulting impedance matrix.

The use of complex permeability allows the influence of proximity effects between adjacent conductors to be captured without explicitly solving for non-uniform current distributions within each conductor. At higher frequencies, the reduced penetration depth of the magnetic field leads to a pronounced diamagnetic behavior of conductors, effectively decreasing the leakage inductance while simultaneously increasing resistive losses. As a result, both the damping of transient oscillations and the resonance frequencies of the winding are correctly reproduced.

To calculate the impedance matrix, the winding is discretized into a number of elements, and the self- and mutual impedances of these elements are calculated based on their geometrical arrangement and material properties. For a given angular frequency ω, the impedance matrix Z(ω) is expressed as

$$Z(\omega) = R(\omega) + j\omega L(\omega) \tag{2}$$

where R(ω) and L(ω) are the frequency-dependent resistance and inductance matrices, respectively. These matrices are obtained from electromagnetic field calculations in which the complex permeability is used to describe both the winding conductors and the magnetic core limb.

The self/mutual impedances can be calculated using the complex linkage flux of the elements. The mean value of the complex magnetic flux crossing element *j* can be obtained by [14]:

$$\phi_j^* = \frac{1}{S_j} \iint_{S_j} \vec{A} \cdot d\vec{S} \tag{3}$$

The mutual flux linkage produced in element *j* (with $I_j = 0$) as a result of a current $I_i$ flowing in element *i* is expressed as:

$$\Phi_{j*} = n_j \phi_{j*} = (-L_{ij} + j\, R\omega_{ij}) I_i \tag{4}$$

Based on this formulation, the inductive and resistive compo-


Morteza Eslamian, Ebrahim Rahimpour, Kabir Sethi, An Investigation on the Effect of Frequency Dependent Inductance Calculation on High Frequency Modeling of Transformer Winding, Journal of Energy, vol. 75 Number 3 (2026), 12–28
https://doi.org/10.37798/2026753754
© 2026 Copyright for this paper by authors. Use permitted under Creative Commons Attribution-NonCommercial (CC BY-NC) 4.0 International License

nents reflected by the magnetic flux can be determined using the following expressions:

$$L_{ij} = -n_i n_j \mathrm{Re}(\phi_j^*)/I_i \quad (5)$$

$$R_{ij} = \frac{\omega\, n_i n_j\, \mathrm{Im}(\phi_j^*)}{I_i} \quad (6)$$

Here, $n_i$ and $n_j$ denote the number of turns associated with elements *i* and *j*, respectively. The resulting frequency-dependent mutual impedance between two representative branches, obtained using this methodology, is presented in Fig. 1.

Impedance matrices are calculated at discrete frequencies of interest and can be directly employed in frequency-domain analyses by interpolating across the whole frequency range, or used to derive constant-inductance models by selecting the impedance matrix at a representative frequency. In the previous work by the authors the former approach was investigated and validated through comparisons with measurements. In the present work, the latter approach is adopted, enabling efficient time-domain simulations while implicitly incorporating frequency-dependent effects relevant to the frequency range of the excitation waveform under consideration.

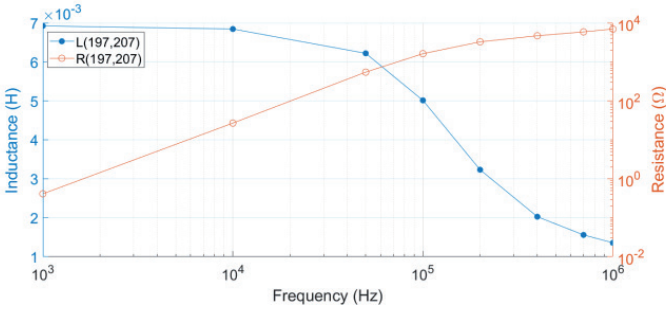


Fig. 1. The frequency dependent mutual impedance of two branches.

## III. Capacitance Calculation

In addition to the winding impedance, an accurate transient model requires proper representation of the capacitive couplings within and around the winding structure. These capacitances play a dominant role in determining the initial voltage distribution and high-frequency resonance behavior of transformer windings. The capacitive network of the winding is represented by a combination of series and shunt capacitances. Series capacitances represent the electrostatic energy stored inside the winding elements (e.g., turns

Table I

Series Capacitance Relations

| **Capacitance** | **Formulation** | **Considerations** |
|---|---|---|
| Turn-to-turn capacitance | $C_{tt} = \frac{\varepsilon_0 \varepsilon_p \pi\, D_m (h + t_p)}{t_p}$ | The term $t_p$ has been added to the conductor's width to consider the fringing effect at conductor edges. |
| Disk-to-disk capacitance | $C_{dd} = \frac{\varepsilon_0 \pi\, D_m (R + t_s)}{\frac{t_p}{\varepsilon_p} + \frac{t_s}{\varepsilon_d}}$ | The term $t_s$ is added to R to consider the fringing effects at disk corners. |
| Series capacitance of an ordinary disk pair | $C_s = \left(\frac{2}{3}\right) C_{dd} + \left(\frac{1}{2}\right)\left(\frac{N_D - 1}{N_D^2}\right) C_{tt}$ | Derived based on a linear voltage distribution and considering the equipotential surfaces between two consecutive disks. |
| Series capacitance of an ordinary disk pair adjacent to a shield ring from top or bottom | $C_s = \left(\frac{1}{2}\right) C_{dd} + \left(\frac{1}{12}\right) C_{ds} + \left(\frac{1}{2}\right)\left(\frac{N_D - 1}{N_D^2}\right) C_{tt}$ | $C_{ds}$ represents the disk-to-shield ring capacitance calculated using the relation of $C_{dd}$ with $t_s$ equal to the distance between the disk and shield ring. |
| Series capacitance of shielded disks | $C_s = \left(\frac{2}{3}\right) C_{dd} + \left(\frac{1}{2}\right)\left(\frac{N_D - k - 1}{N_D^2}\right) C_{tt} + \left(\frac{k}{2}\right) C_{sh} \left(2 + \frac{1 - 2N_D}{N_D^2}\right)$ | $C_{sh}$ represents the capacitance between a shield turn and an adjacent disk turn, calculated with a similar approach to that used for $C_{tt}$, utilizing the corresponding value for $t_p$. |
| Equivalent relative permittivity of radial oil ducts | $\varepsilon_d = \frac{n_s b_s}{\pi\, D_m} \varepsilon_s + \left(1 - \frac{n_s b_s}{\pi\, D_m}\right) \varepsilon_o$ | The equivalent relative permittivity of the axial oil ducts can be calculated in a similar manner, where $n_s$ and $b_s$ denote the corresponding rib parameters. |

Parameter definition:
$\varepsilon_0$: permittivity of free space
$\varepsilon_p$: relative permittivity of paper insulation
$\varepsilon_s$: relative permittivity of spacer
$\varepsilon_d$: equivalent relative permittivity of radial canal between disks
$D_m$: average diameter of winding
h: bare height of the conductor
$t_p$: total paper insulation thickness (both sides)
R: winding's radial depth
$t_s$: thickness of the solid insulation (radial spacers) between disks
$N_D$: disk's turns number
k: number of shield turns per disk
$n_s$: number of spacers between disks
$b_s$: width of a spacer between disks

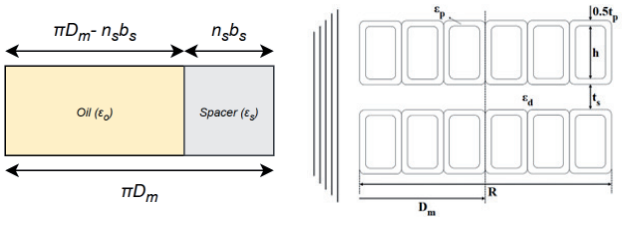




Morteza Eslamian, Ebrahim Rahimpour, Kabir Sethi, An Investigation on the Effect of Frequency Dependent Inductance Calculation on High Frequency Modeling of Transformer Winding, Journal of Energy, vol. 75 Number 3 (2026), 12–28
https://doi.org/10.37798/2026753754
© 2026 Copyright for this paper by authors. Use permitted under Creative Commons Attribution-NonCommercial (CC BY-NC) 4.0 International License

or discs), while shunt capacitances represent the coupling between winding elements and grounded surfaces, such as the transformer core, tank, and electrostatic shields.

The capacitance matrix remains approximately frequencyindependent within the frequency range relevant to fast transient studies, and therefore constant capacitance values are used throughout the present analysis. Although local dielectric losses may introduce minor frequency dependence at very high frequencies, their influence on voltage distribution is generally negligible compared to that of inductive and resistive effects.

### *A. Series Capacitance Calculation*

Series capacitances of winding elements are calculated based on the geometry of adjacent conductors and the dielectric properties of the intervening insulation [18]. The capacitance relations used for this study are provided in Table I. Considering the equipotential lines between adjacent discs, the equivalent series capacitance of a disc pair can be formulated as the sum of two separate terms representing, respectively, the electrostatic energy stored between the conductors inside the discs and the energy stored in the space between the discs.

In end discs, it is very common to use shield rings to reduce electrical stresses at the winding corners. When a disc pair is located above or below a shield ring, the expression for the equivalent series capacitance can be suitably modified to account for the energy stored in the space between the disc and the adjacent shield ring. An important technique for achieving a more uniform voltage distribution and reducing stress in the initial discs of the winding is to increase the equivalent series capacitance by employing shield conductors between the inner turns of the discs. This practice increases the voltage between adjacent conductors and consequently raises the total electrostatic energy stored. In this case, the term corresponding to the energy stored between the conductors and the shields becomes the dominant contributor to the equivalent series capacitance.

It is also worth noting that if a shield ring is situated above or below a shielded disc pair, the same type of correction introduced for a normal disc pair can likewise be applied here. When calculating the capacitance between two discs, an appropriate equivalent relative permittivity is used to account for the non-homogeneous dielectric properties of the oil ducts. For layer-type windings, it is sufficient to assume a disc turn number equal to one in the relation for series capacitances. In this case, the term associated with the internal energy of the discs becomes zero, and only the capacitance related to the turn-to-turn axial energy is considered in the calculations.

### *B. Parallel Capacitance Calculation*

These capacitances represent the coupling between adjacent windings or between a winding and grounded components such as the core limb or the tank. The total parallel capacitance between two concentric windings is distributed proportionally among the winding elements along the axial duct. Similarly, the calculated ground capacitances of the innermost and outermost windings are allocated to the winding elements in proportion to their respective heights.

- Parallel Capacitance Between Windings

The parallel capacitance between two windings is calculated using the expression for two concentric cylinders:

$$C_p = \frac{\varepsilon_0 \pi D_m H}{\frac{t_o}{\varepsilon_o} + \frac{t_p}{\varepsilon_p}} \tag{7}$$

where $D_m$ is the mean diameter of the gap between the windings, $t_o$ and $t_p$ are the thicknesses of the oil and solid insulation between the windings, respectively, and $H$ is the average winding height. To account for the presence of axial spacers or ribs located between barrier cylinders, an equivalent relative permittivity is calculated similar to one used for the equivalent relative permittivity of radial oil ducts as given in Table 1.

- Ground Capacitance of the Innermost Winding

The capacitance between the innermost winding and the core limb is calculated using the same approach as for the parallel capacitance between two windings, following equation (7). In this case, the height $H$ corresponds to the height of the innermost winding, typically multiplied by a factor of 1.1 or 1.2 to account for fringing effects.

- Ground Capacitance of the Outermost Winding

The capacitance between the outermost winding and the tank wall can be estimated using the formula for a cylindrical conductor positioned near a ground plane. However, due to challenges associated with the finite dimension of the tank walls and the complex geometry involved, this capacitance is typically determined through direct measurements on the transformer's active part rather than analytical calculations.

## IV. Calculation of System Response

The overall impedance matrix for the equivalent circuit is derived once the individual capacitances and impedances of the network are determined. This process begins with calculating the system admittance matrix, $Y_{sys}(\omega)$, using the following relationship:

$$Y_{sys}(\omega) = Y(\omega) + A[Z(\omega)]^{-1}A^T \tag{8}$$

where $Y(\omega)$ is the network admittance matrix, $Z(\omega)$ is the branch impedance matrix, and $A$ is the node-branch incidence matrix.

The network admittance matrix is defined as:

$$Y(\omega) = j\omega C + G(\omega) \tag{9}$$

In this expression, $C$ refers to the nodal capacitance matrix, while $G(\omega)$ is the conductance matrix accounting for dielectric losses within the windings. For the purposes of this specific study, dielectric losses are considered negligible and are omitted from the simulations ($G \approx 0$).

To obtain the system impedance matrix, $Z_{sys}(\omega)$, the admittance matrix is inverted:

$$Z_{sys}(\omega) = [Y_{sys}(\omega)]^{-1} \tag{10}$$

Once $Z_{sys}(\omega)$is determined, it is utilized to find the voltage transfer function from input node $i$ to output node $j$ as follows:

$$T_{j,i}(\omega) = \frac{Z_{ji}(\omega)}{Z_{ii}(\omega)} \tag{11}$$

To simulate the transient response, consider a voltage $v_i(t)$ applied to node $i$ of the winding. By applying the Inverse Fast Fourier Transform (IFFT), the voltage response at node $j$ is given by:

$$v_j(t) = \text{IFFT}(V_i(\omega) \cdot T_{j,i}(\omega)) \text{ where } V_i(\omega) = \text{FFT}(v_i(t)) \tag{12}$$

represents the transformation of the input voltage into the frequency domain.


Morteza Eslamian, Ebrahim Rahimpour, Kabir Sethi, An Investigation on the Effect of Frequency Dependent Inductance Calculation on High Frequency Modeling of Transformer Winding, Journal of Energy, vol. 75 Number 3 (2026), 12–28
https://doi.org/10.37798/2026753754
© 2026 Copyright for this paper by authors. Use permitted under Creative Commons Attribution-NonCommercial (CC BY-NC) 4.0 International License

## V. Test Object and Measurement

The test object is a single unit of a three-winding power transformer rated at 250 MVA with nominal voltage levels of 525/154/66 kV and a YNynd vector group configuration, as illustrated in Fig. 2. To enable access to the high-voltage (HV) main winding, the upper yoke of the EY-type magnetic core was removed and the regulating windings were temporarily taken out.

All measurements were carried out with the transformer in a test-ready condition, where the active part was exposed to air and the unit was no longer oil-immersed. The HV winding is implemented as a center-entry disk winding and incorporates shielding disks to improve the uniformity of impulse voltage distribution. It comprises 168 disks arranged into 84 branches, with two disks per branch. The medium-voltage (MV) winding is similarly of disk-type construction and consists of 150 disks grouped into 75 branches. The tertiary-voltage (TV) winding is designed as a helical layer winding, containing 158 turns divided into 79 branches, with two turns per branch .For the purpose of electrical measurements, sections of the insulation paper were carefully removed, and the enamel coating on the conductor surfaces was stripped. This preparation ensured reliable electrical contact between the measurement probes and the conductors during the tests.

### *A. RSO Measurement*

The Recurrent Surge Oscillation (RSO) test is a diagnostic method used to evaluate voltage stress distribution in transformer windings during impulse and transient conditions. In this test, a low-voltage impulse, typically a few hundred volts, is applied to the winding, and the resulting voltage distribution is recorded as a percentage of the applied impulse, providing an indication of the expected behavior under standard lightning impulse conditions. Because RSO measurements are usually performed in air, direct comparison with full-scale lightning impulse tests can be challenging. The transient voltage distribution is highly dependent on the dielectric permittivity, which varies with insulation moisture and temperature. Therefore, these parameters must be estimated accurately to ensure meaningful interpretation.

The test setup consists of a recurrent surge generator, a two-channel digital oscilloscope, and two calibrated low-capacitance (typically <10 pF) passive voltage probes.



Fig. 2. A single unit of the tested 250 MVA transformer

The procedure begins with probe calibration, after which one probe records the applied impulse and the other measures the voltage response at the selected point. Lead lengths should be minimized to avoid parasitic inductive effects. The generator is then adjusted to produce a waveform close to the standard impulse shape. Both applied and response waveforms are captured simultaneously, typically over a 400–800 μs time window. A sampling frequency of at least 10 MHz is required to reliably capture the wavefront and any chopping phenomena.

### *B. FRA Measurement*

The FRA test setup consists of an FRA analyzer capable of generating a controlled wide-band excitation (typically from 20 Hz up to several MHz) and coaxial cables with consistent characteristic impedance. Prior to testing, the measurement system must be calibrated, including verification of cable integrity and compensation for stray impedances. Measurements are performed using the sweep-frequency method, in which a low-voltage sinusoidal signal is injected into the winding while the voltage response is simultaneously recorded at the output point. The ratio of output to input gives the complex transfer function over the entire frequency band.

Care must be taken to ensure proper grounding, minimize cable lengths, and avoid creating unintended loops that could introduce parasitic inductances or alter the measurement accuracy. The test configuration should strictly follow standardized procedures, such as those defined in IEC 60076-18 [19] or Cigré WG A2/26 [20].

Accurate interpretation of FRA results requires consideration of environmental and dielectric conditions. The frequency response is affected by factors such as insulation moisture content, oil temperature, and the dielectric constant of the surrounding medium. For test objects that are not oil-immersed, such as transformers under refurbishment or laboratory investigation, the altered dielectric environment must be taken into account when evaluating the resonance patterns and amplitude levels. It should be noted that in FRA tests, a 50-ohm resistance is typically connected between the output point and ground which should be also taken into account in the simulations.

## VI. Simulation Results and Discussions

The detailed transformer winding model presented in the previous section was constructed and analyzed after calculating the required capacitive and inductive parameters. A detailed depiction of the windings is provided in Fig. 3. The model comprises 238 branches, each defined by a self-impedance as well as mutual impedances with all other elements. The node numbers corresponding to the winding terminals, along with the output nodes used for evaluating voltage responses, are shown in Fig. 4. For the frequency-dependent model, a frequency-varying impedance matrix is used, which includes the self and mutual inductances and resistances interpolated over the whole frequency range.

For the constant-inductance models, the general approach for analyzing the system equations in the frequency-domain is still used, with the difference that the imaginary part of the impedance matrix is replaced by a constant inductance matrix. However, to represent the damping, the real part of the frequency-varying impedance matrix is used. In this way, both constant- and variable-inductance models have identical damping, which allows better and easier comparison across the entire frequency range.

The voltage response at various winding nodes under input voltages used in the RSO test was simulated and compared with measurement results. Calculations were performed separately for inductance matrices determined at different frequencies.


Morteza Eslamian, Ebrahim Rahimpour, Kabir Sethi, An Investigation on the Effect of Frequency Dependent Inductance Calculation on High Frequency Modeling of Transformer Winding, Journal of Energy, vol. 75 Number 3 (2026), 12–28
https://doi.org/10.37798/2026753754
© 2026 Copyright for this paper by authors. Use permitted under Creative Commons Attribution-NonCommercial (CC BY-NC) 4.0 International License

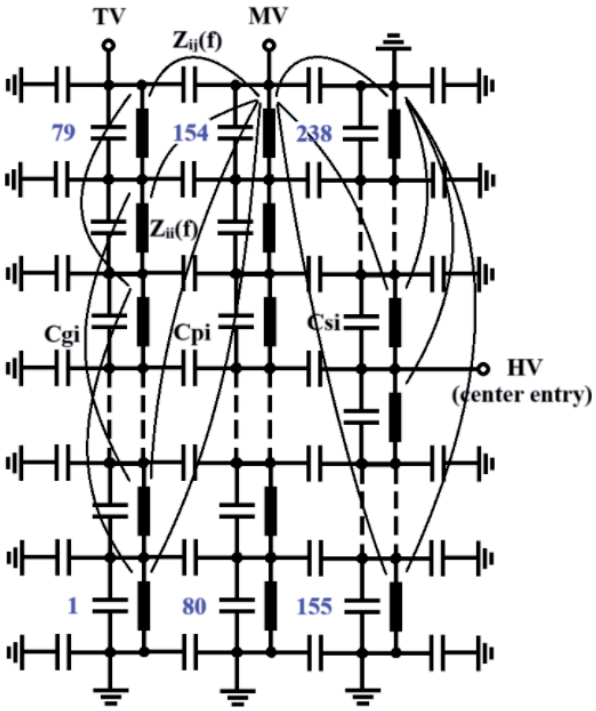


Fig. 3. Transformer equivalent circuit

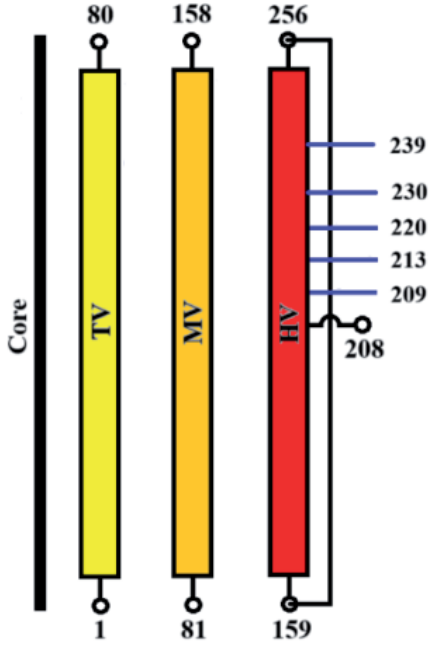


Fig. 4. Input and output node numbers

As can be seen from Fig. 5, for the full impulse wave input, the response computed at 0 Hz shows considerable discrepancies in the oscillations of the voltage waveforms compared with the measurements. As the frequency used to determine the inductance matrix increases, the time-domain waveforms shift to the left along the time axis, and the differences relative to the measurements decrease. At 100 kHz, a good agreement between measured and simulated results is achieved. Further increasing the frequency to 1 MHz shifts the waveforms even further to the left and again leads to a slight increase in the discrepancies.

The voltage response calculated using the frequency-varying inductance matrix (frequency-dependent model) is also shown in Fig. 5. The frequency-varying inductance matrix is obtained by interpolating the inductance matrices computed at different frequencies in the range of 1 kHz to 1 MHz. As also discussed in the previous work [8], this model produces the closest output to the measurements and offers high accuracy. It can be observed that, although the 100-kHz model still has lower accuracy than the frequency-dependent model, it performs much better than the other single-frequency models and especially better than the 0-Hz model, which is also the commonly used analytical model. Fig. 6 shows the simulation and measurement results for the chopped impulse wave input. Similar to the previous case, the 0-Hz model


Morteza Eslamian, Ebrahim Rahimpour, Kabir Sethi, An Investigation on the Effect of Frequency Dependent Inductance Calculation on High Frequency Modeling of Transformer Winding, Journal of Energy, vol. 75 Number 3 (2026), 12–28
https://doi.org/10.37798/2026753754
© 2026 Copyright for this paper by authors. Use permitted under Creative Commons Attribution-NonCommercial (CC BY-NC) 4.0 International License

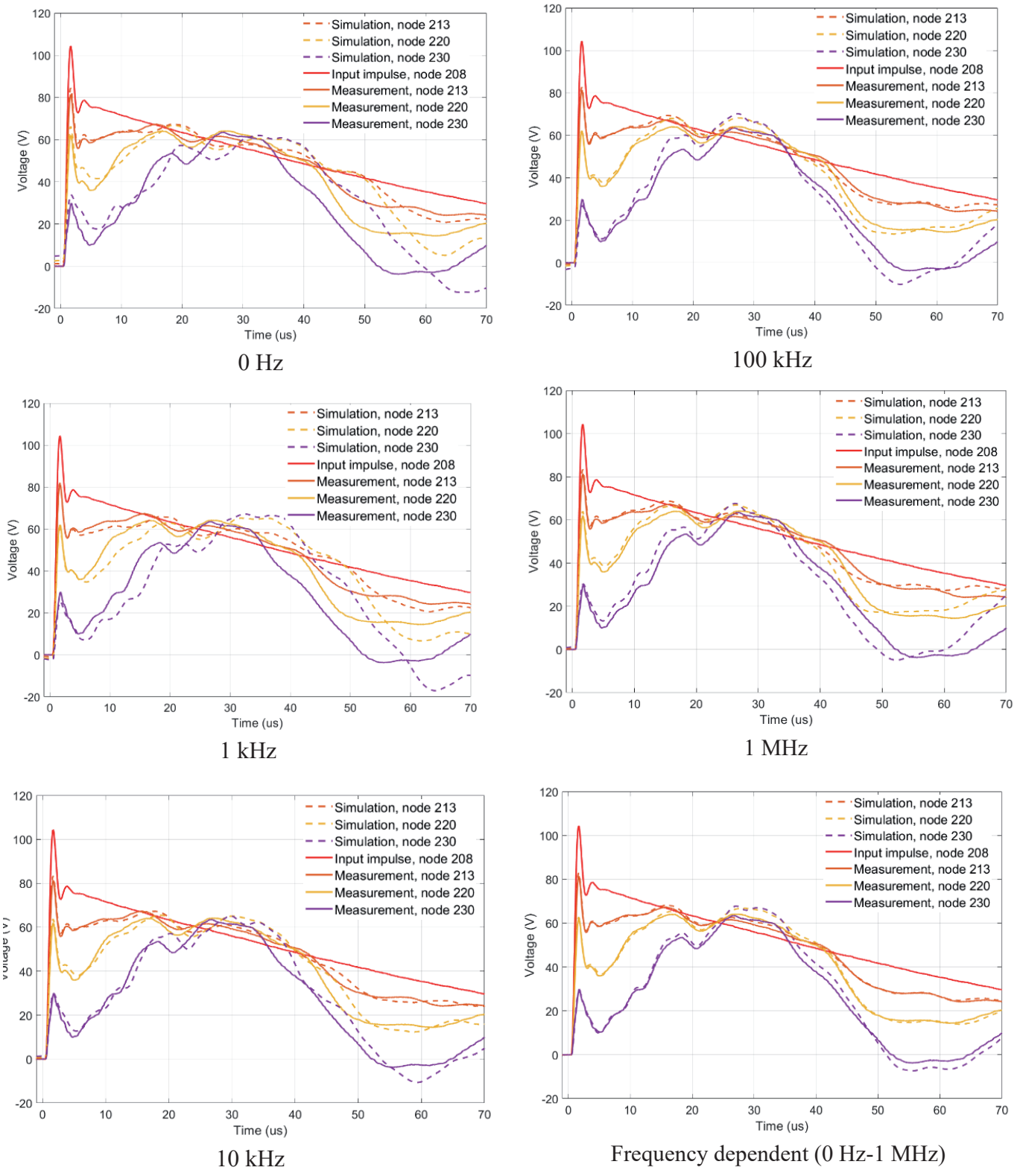


Fig. 5. Voltage response at different nodes for full impulse input with different frequency-varying inductance matrices

exhibits significant errors in the post chopping oscillations. As the frequency increases from 0 Hz to 100 kHz, the accuracy improves, and the post chopping oscillations become closer to the measured results. Increasing the frequency further to 1 MHz appears to shift the waveforms too far to the left in the time domain, again increasing the discrepancies. It is worth noting that the frequency-dependent model still offers the highest accuracy, but among the constant-inductance models, the 100-kHz inductance matrix yields the closest results to the measurements.

To gain better insight into the winding models, frequency-domain responses at the same output points were also simulated and compared with the FRA measurement. The frequency response of the voltage for the constant-inductance models as well as the frequency-dependent model is shown in Fig. 7. It can be observed that the greatest error corresponds to the model with the 0-Hz inductance matrix. Using inductance matrices computed at higher frequencies improves accuracy, and at 100 kHz the discrepancies become minimal and the agreement with measurements especially in the range of several ten kHz to several hundred kHz is remarkable.


Morteza Eslamian, Ebrahim Rahimpour, Kabir Sethi, An Investigation on the Effect of Frequency Dependent Inductance Calculation on High Frequency Modeling of Transformer Winding, Journal of Energy, vol. 75 Number 3 (2026), 12–28
https://doi.org/10.37798/2026753754
© 2026 Copyright for this paper by authors. Use permitted under Creative Commons Attribution-NonCommercial (CC BY-NC) 4.0 International License

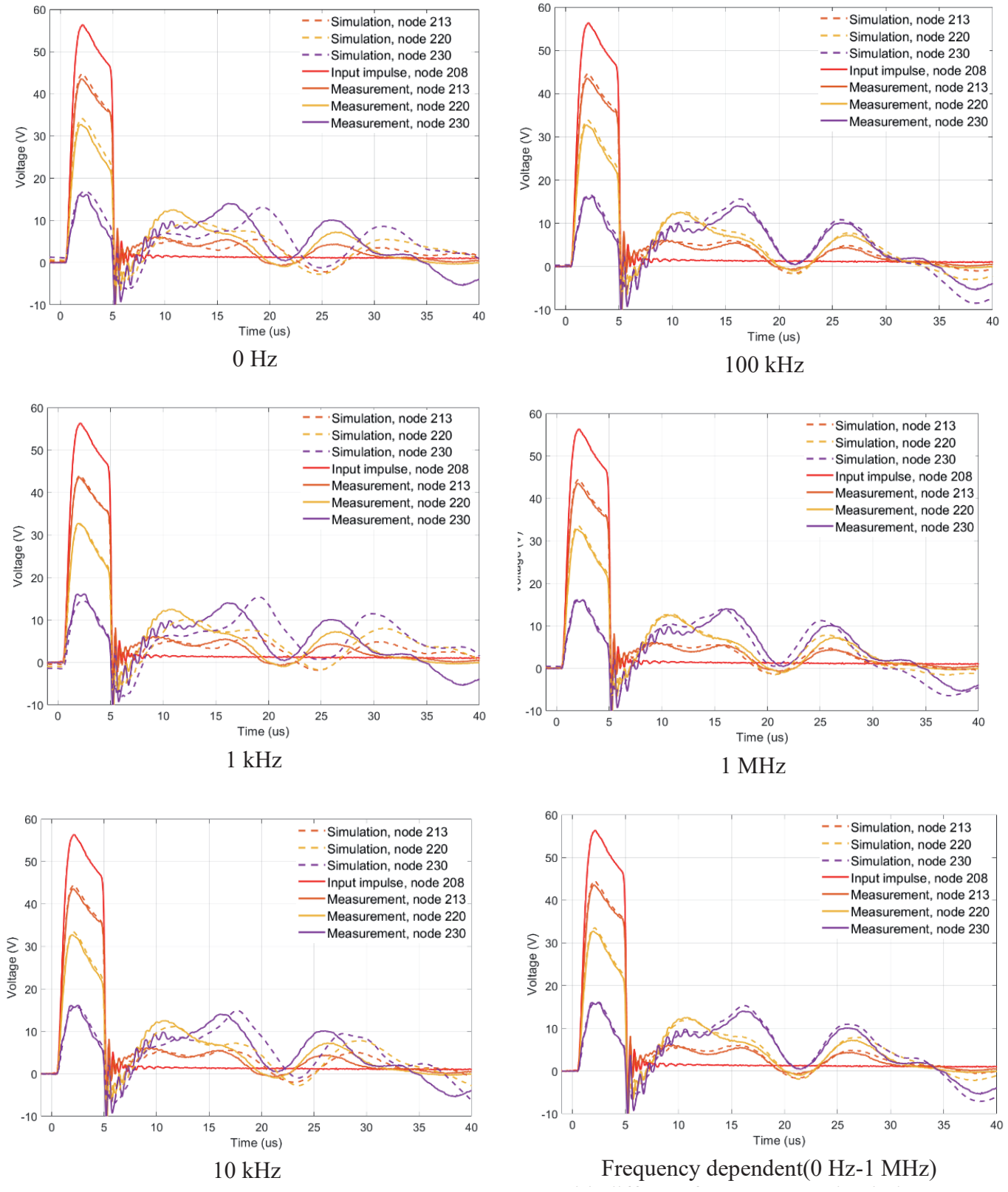


Fig. 6. Voltage response at different nodes for chopped impulse input with different frequency-varying inductance matrices

Increasing the frequency beyond this does not help and even slightly increases the discrepancies. These observations are fully consistent with the time-domain results. It should also be noted that, in contrast to the time domain, increasing the frequency causes the curves to shift to the right along the frequency axis. Again, it is emphasized that the frequency-dependent model, which uses a frequency-varying inductance matrix, maintains the highest accuracy across the entire frequency range compared with all constant-inductance models.

Based on the above discussion, it can be concluded that accurately modeling winding behavior still requires a frequency-dependent model. However, it is possible to obtain acceptable results using a constant-inductance model by replacing the 0-Hz inductance matrix with one computed at a higher frequency that effectively captures frequency-dependent effects. Clearly, the appropriate frequency for calculating the inductance matrix depends on the frequency range excited by the applied input. The results of this


Morteza Eslamian, Ebrahim Rahimpour, Kabir Sethi, An Investigation on the Effect of Frequency Dependent Inductance Calculation on High Frequency Modeling of Transformer Winding, Journal of Energy, vol. 75 Number 3 (2026), 12–28
https://doi.org/10.37798/2026753754
© 2026 Copyright for this paper by authors. Use permitted under Creative Commons Attribution-NonCommercial (CC BY-NC) 4.0 International License

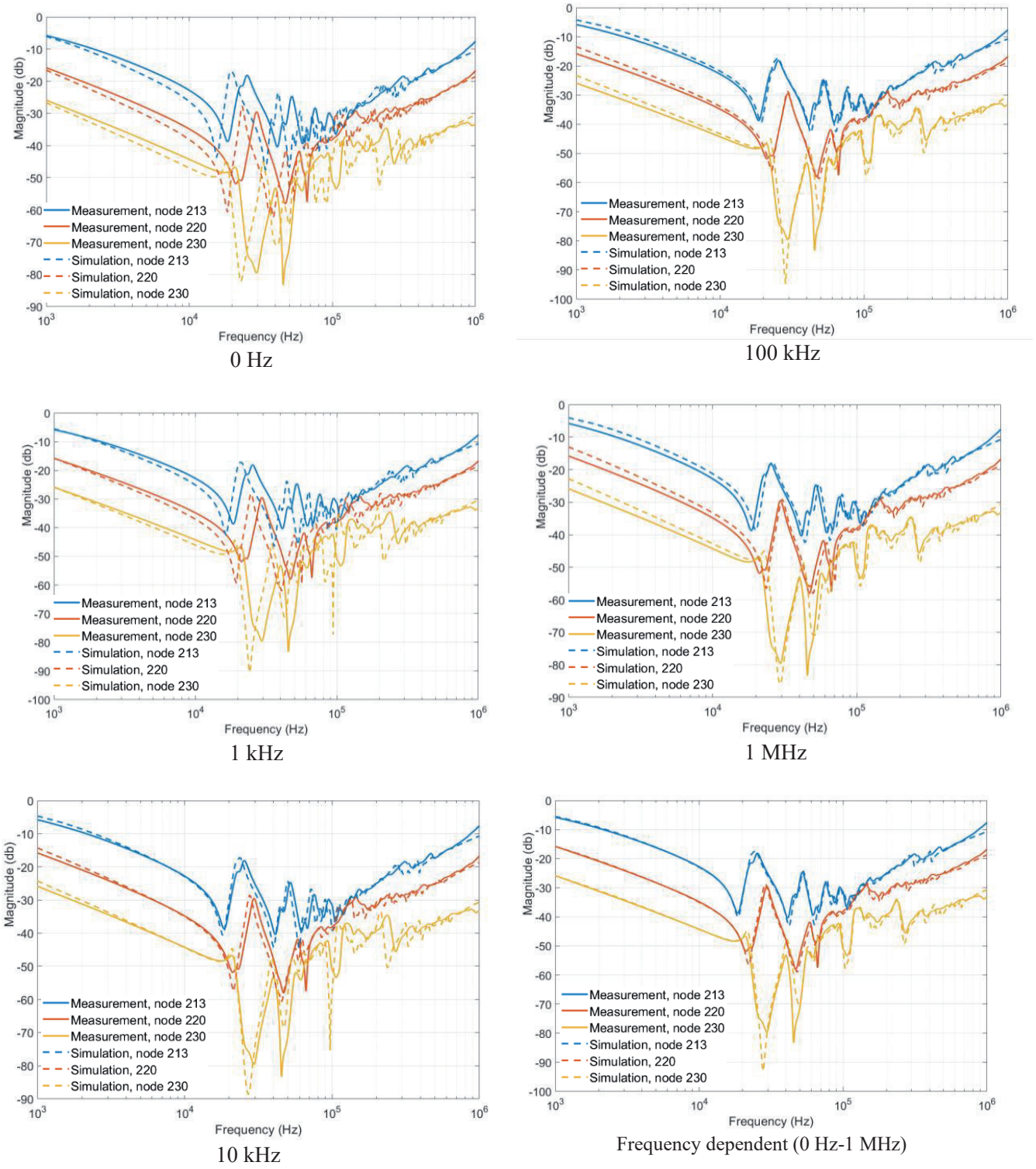


Fig. 7. Voltage transfer function at different nodes with different frequency-varying inductance matrices

study show that 100 kHz provides the best results for both full and chopped impulses, as confirmed by comparisons in both the time and frequency-domains. As mentioned earlier, constant-inductance models have the advantage of being directly solvable in the time domain, enabling the study of the effects of adding nonlinear elements such as surge arresters as an effective means of limiting internal overvoltages, particularly at the outputs of regulating windings. The results demonstrate that inductances calculated at appropriately selected higher frequencies lead to a substantial improvement in accuracy.


Morteza Eslamian, Ebrahim Rahimpour, Kabir Sethi, An Investigation on the Effect of Frequency Dependent Inductance Calculation on High Frequency Modeling of Transformer Winding, Journal of Energy, vol. 75 Number 3 (2026), 12–28
https://doi.org/10.37798/2026753754
© 2026 Copyright for this paper by authors. Use permitted under Creative Commons Attribution-NonCommercial (CC BY-NC) 4.0 International License

## VII. Conclusion

In this paper, the high-frequency behavior of a three-winding transformer is investigated. Time- and frequency-domain simulations are performed and compared with RSO and FRA measurement results. The frequency-dependent effects of transformer windings, including skin and proximity effects, have a significant influence on the frequency and magnitude of internal resonances. Simulations show that neglecting these effects leads to considerable discrepancies in the voltage response in both the time and frequency domains. The fundamental solution is to use a frequency-dependent model with a frequency-varying inductance matrix. Although this model provides high accuracy, it requires analysis in the frequency-domain, which introduces limitations when nonlinear elements such as surge arresters need to be incorporated. In contrast, constant-inductance models can be solved directly in the time domain, offering significantly faster computation of transient voltages. However, their main drawback is the inadequate representation of the frequency-dependent effects inside the windings. This study demonstrates that the accuracy of the constant-inductance model can be improved by replacing the zero-frequency inductance matrix with an inductance matrix calculated at a higher frequency. The appropriate frequency depends on the spectral content of the applied waveform. The results presented in this paper indicate that, for both full and chopped impulse inputs, the inductance matrix calculated at 100 kHz provides a better agreement with the measurement results compared with the other evaluated frequencies.

## References


[1] JWG A2/C4.52, High-Frequency Transformer and Reactor Models for Network Studies – Part A: White-Box Models, CIGRE Technical Brochure 900, 2023. ISBN 978-2-85873-605-8.

[2] E. E. Mombello and G. A. Díaz Flórez, "An improved high frequency white-box lossy transformer model for the calculation of power systems electromagnetic transients," Electric Power Systems Research, vol. 190, p. 106838, Jan. 2021.

[3] M. Popov, "General approach for accurate resonance analysis in transformer windings," Electric Power Systems Research, vol. 161, pp. 45–51, 2018.

[4] Z. Luna, P. Gómez, F. P. Espino-Cortés, and R. Peña-Rivero, "Modeling of Transformer Windings for Fast Transient Studies: Experimental Validation and Performance Comparison", IEEE Transactions on Power Delivery, Vol. 32, No. 4, pp. 1852-1860, 2017.

[5] M. Eslamian, and B. Vahidi, "New Equivalent Circuit of Transformer Winding for the Calculation of Resonance Transients Considering Frequency-Dependent Losses", IEEE Tractions on Power Delivery, Vol. 30, No. 4, pp. 1743-1751, 2015.

[6] E. E. Mombello, "New Compact White-Box Transformer Model for the Calculation of Electromagnetic Transients", IEEE Transactions on Power Delivery, Vol. 37, No. 4, pp. 2921-2931, 2022.

[7] M. Eslamian, M. Bigdeli, A. Abu-Siada, "High frequency modelling of dry type detuned reactor for transient studies: Simulation and experimental analyses," Electric Power Systems Research, vol. 228, pp. 110102, 2024.

[8] M. Eslamian, K. Sethi, M. Habukawa, K. Yamaguchi, "An Investigation on Frequency Response Analysis of a Large 250 MVA Three-Winding Transformer: High-Frequency Modelling Approach vs. FRA Measurements," CIGRE SC A2&D1 Joint Colloquium, Oct. 27–Nov. 1, Seoul, Korea, 2025.

[9] M. Gunawardana, F. Fattal, B. Kordi, "Very Fast Transient Analysis of Transformer Winding Using Axial Multiconductor Transmission Line Theory and Finite Element Method", IEEE Transactions on Power Delivery, Vol. 34, No. 5, pp. 1948-1956, 2019.

[10] B. Gustavsen, "Wide band modelling of power transformers," IEEE Transactions on Power Delivery, Vol. 19, No. 1, pp. 414–422, 2004.

[11] JWG A2/C4.52, High-Frequency Transformer and Reactor Models for Network Studies – Part B: Black-Box Models, CIGRE Technical Brochure 901, 2023. ISBN 978-2-85873-606-5.

[12] JWG A2/C4.52, High-Frequency Transformer and Reactor Models for Network Studies – Part C: Grey-Box Models, CIGRE Technical Brochure 902, 2023. ISBN 978-2-85873-602-2.

[13] D. J. Wilcox, M. Conlon and W. G. Hurley, "Calculation of self and mutual impedances for coils on ferromagnetic cores," IEE Proc. Science, Measurement and Technology, Vol. 135, No. 7, pp. 470-476, 1988.

[14] O. Moreau, L. Popiel, J. L. Pages, "Proximity losses computation with a 2D complex permeability modelling", IEEE Transactions on Magnetics", Vol. 34, No. 5, pp. 3616-3619, 1998.

[15] A. D. Podoltsev, K. G. N. B. Abeywickrama, Y. V. Serdyuk, and S. M. Gubanski, "Multiscale Computations of Parameters of Power Transformer Windings at High Frequencies. Part II: Large-Scale Level", IEEE Transactions on Magnetics", Vol. 43, No. 12, pp. 4076-4082, 2007.

[16] N. Abeywickrama, Y. V. Serdyuk, and S. M. Gubanski, "Highfrequency modelling of power transformers for use in frequency response analysis (FRA)," IEEE Transactions on Power Delivery, vol. 23, no. 4, pp. 2042– 2049, 2008.

[17] S. D. Mitchell and J. S. Welsh, "The Influence of Complex Permeability on the Broadband Frequency Response of a Power Transformer," IEEE Transactions on Power Delivery, Vol. 25, No. 2, pp. 803-813, 2010.

[18] S. V. Kulkarni, and S. A. Khaparde, "Transformer Engineering Design, Technology and Diagnostics", Second Edition Taylor & Francis Group, 2013.

[19] IEC 60076-18, "Power transformers – Part 18: Measurement of frequency response", 2012

[20] Cigré WG A2/26, "Mechanical condition assessment of transformer windings using Frequency Response Analysis (FRA)", Brochure 342, Paris 2008




Morteza Eslamian, Ebrahim Rahimpour, Kabir Sethi, An Investigation on the Effect of Frequency Dependent Inductance Calculation on High Frequency Modeling of Transformer Winding, Journal of Energy, vol. 75 Number 3 (2026), 12–28
https://doi.org/10.37798/2026753754
© 2026 Copyright for this paper by authors. Use permitted under Creative Commons Attribution-NonCommercial (CC BY-NC) 4.0 International License